Supplementary Material for "Combining Feature Correspondence with Parametric Chamfer Alignment: Hybrid Two-Stage Registration for Ultra-Widefield Retinal Images"

Li Ding, *Student Member, IEEE*, Tony D. Kang, Ajay E. Kuriyan, Rajeev S. Ramchandran, Charles C. Wykoff, and Gaurav Sharma, *Fellow, IEEE*

S.I. Overview

This document provides Supplementary Material for the paper [1]. In Section S.II, we present the least squares estimation for the global transformation parameters $\boldsymbol{\beta}$ for different order polynomial transformation. In Section S.III, we provide details of the EM-based chamfer alignment algorithm used in the second stage of our proposed hybrid registration algorithm by deriving the expressions for posterior probabilities and the parameter updates. Finally, in Section S.IV, we show larger images corresponding to entire registered vessel maps for the proposed and alternative techniques; smaller regions from these are included in the main paper.

S.II. Least Squares Parameter Estimates for the Global Registration Transform

The polynomial transformation parameters $\boldsymbol{\beta}$ used for the global geometric transform in Section II-A of the main manuscript are obtained via a least-squares procedure that we outline in this section. The geometric transformation from the target to the reference spatial coordinates is defined in terms of a polynomial in the variables x and y, as

$$\psi_M([x,y]^\intercal,\boldsymbol{\beta}) = \sum_{m=0}^{M}\sum_{i=0}^{m}\beta_{m,i}x^{m-i}y^i \stackrel{\text{def}}{=} \boldsymbol{\beta}_M^\intercal \mathbf{a}([x,y]^\intercal), \tag{S.1}$$

$$\boldsymbol{\beta}_M = [\beta_{0,0},\beta_{1,0},\beta_{1,1},\beta_{2,0},\beta_{2,1},\ldots,\beta_{M,M}]^\intercal, \tag{S.2}$$

$$\mathbf{a}([x,y]) = \left[1,x,y,x^2,xy,\ldots,y^M\right]^\intercal, \tag{S.3}$$

where M is the order of the polynomial and $\beta_{m,i}, m=0\ldots M, i=0\ldots m$ denote the $(M+1)(M+2)/2$ coefficients of the polynomial. In terms of the polynomial in (S.1), we can then express the M-th order polynomial geometric transformation as

$$\bar{\mathcal{T}}_{\boldsymbol{\beta}_M}\left(\mathbf{p}^{(t)}\right) = \boldsymbol{\beta}_M^\intercal \mathbf{a}(\mathbf{p}^{(t)}), \tag{S.4}$$

where $\mathbf{p}^{(t)}$ and $\bar{\mathcal{T}}_{\boldsymbol{\beta}_M}\left(\mathbf{p}^{(t)}\right)$ are 2×1 coordinate vectors denoting corresponding spatial locations in the target and reference images, respectively, $\boldsymbol{\beta}_M = [\boldsymbol{\beta}_M^u, \boldsymbol{\beta}_M^v]$ denotes the matrix whose columns $\boldsymbol{\beta}_M^u$ and $\boldsymbol{\beta}_M^v$ are the parameter vectors for M-th order polynomial transformations corresponding to the two spatial coordinates in the reference image space, denoted by u and v, respectively.

Given N pairs of matched feature points $\mathbf{p}_n^{(r)} = (u_n, v_n)^\intercal$ and $\mathbf{p}_n^{(t)} = (x_n, y_n)^\intercal$ in the reference and target images, respectively, we would like to determine the optimal transformation parameters $\boldsymbol{\beta}_M^*$ such that the transformed target coordinates closely approximate their corresponding reference points, i.e., $(\boldsymbol{\beta}_M^*)^\intercal \mathbf{a}_n \approx \mathbf{p}_n^{(r)}$ for $n=1,2,\ldots N$. Least squares estimates are readily obtained as

$$\boldsymbol{\beta}_M^* = \arg\min_{\boldsymbol{\beta}_M} \|\mathbf{A}\boldsymbol{\beta}_M - \mathbf{b}\|^2 = \mathbf{A}^\dagger \mathbf{b}, \tag{S.5}$$

The work was supported in part by a University of Rochester Research Award, by a distinguished researcher award from the New York state funded Rochester Center of Excellence in Data Science (CoE #3B C160189) at the University of Rochester, by an unrestricted grant to the Department of Ophthalmology from Research to Prevent Blindness, and grant P30EY001319-35 from the National Institutes of Health.

L. Ding and G. Sharma are with the Department of Electrical and Computer Engineering, University of Rochester, Rochester, NY 14627, USA (e-mail: {l.ding, gaurav.sharma}@rochester.edu).

T. D. Kang and R. S. Ramchandran are with the University of Rochester Medical Center, University of Rochester, Rochester, NY 14642, USA (e-mail: {tony_kang, rajeev_ramchandran}@urmc.rochester.edu).

A. E. Kuriyan is with the Mid Atlantic Retina, Retina Service of Wills Eye Hospital, Thomas Jefferson University, Philadelphia, PA 19107 & the University of Rochester Medical Center, University of Rochester, Rochester, NY 14642, USA (e-mail: ajay.kuriyan@gmail.com).

C. C. Wykoff is with Retina Consultants of Houston and Blanton Eye Institute, Houston Methodist Hospital & Weill Cornell Medical College, Houston, TX 77030, USA (e-mail: ccwmd@houstonretina.com).

where

$$\mathbf{A} = [\mathbf{a}_1, \mathbf{a}_2, \cdots, \mathbf{a}_N]^\intercal, \tag{S.6}$$

$$\mathbf{b} = \left[\mathbf{p}_1^{(r)}, \mathbf{p}_2^{(r)}, \cdots, \mathbf{p}_N^{(r)}\right]^\intercal, \tag{S.7}$$

and $\mathbf{A}^\dagger$ denotes the pseudo-inverse of $\mathbf{A}$ given by $\mathbf{A}^\dagger = \left(\mathbf{A}^\intercal\mathbf{A}\right)^{-1}\mathbf{A}^\intercal$ for the typical situation where $\left(\mathbf{A}^\intercal\mathbf{A}\right)$ is non-singular.

S.III. Detailed Derivation Of The Parameter Estimation With The EM Algorithm

We describe the computation of the registration parameters for the k^{th} pair of coarsely aligned corresponding reference and target image patches and therefore assume that k is fixed throughout the following description. For the j^{th} vessel pixel $\mathbf{p}_j^{(t,k)}$ in the k^{th} target image patch, the squared chamfer distance $d_j\left(\boldsymbol{\beta}_k\right)$ to the corresponding reference image under the transformation $\tilde{\mathcal{T}}_{\boldsymbol{\beta}_k}\left(\cdot\right)$ is defined as the minimum squared Euclidean distance between the transformed point $\tilde{\mathcal{T}}_{\boldsymbol{\beta}_k}\left(\mathbf{p}_j^{(t,k)}\right)$ and the set of vessel pixel locations $\mathcal{Q}_{r,k}$ for the corresponding reference image, i.e.,

$$d_j\left(\boldsymbol{\beta}_k\right) = \min_i \left\|\mathbf{p}_i^{(r,k)} - \tilde{\mathcal{T}}_{\boldsymbol{\beta}_k}\left(\mathbf{p}_j^{(t,k)}\right)\right\|^2. \tag{S.8}$$

The E-step calculates the expectation of the complete-data log-likelihood

$$\begin{aligned} Q &= \mathbb{E}\left[\sum_{j=1}^{M_{t,k}} \log p\left(d_j, z_j^k | \pi_k, \lambda_k, \boldsymbol{\beta}_k\right)\right] \\ &= \sum_{j=1}^{M_{t,k}} \sum_{z_j^k \in \{0,1\}} p\left(z_j^k | \pi_k, \lambda_k, \boldsymbol{\beta}_k, d_j\right) \log p\left(d_j, z_j^k | \pi_k, \lambda_k, \boldsymbol{\beta}_k\right) \\ &= \sum_{j=1}^{M_{t,k}} p_j^k \left[-\lambda_k d_j + \log\left(\pi_k\right) + \log\left(\lambda_k\right)\right] + \left(1 - p_j^k\right)\left[\log\left(1-\pi_k\right) - \log\left(P\right)\right], \end{aligned} \tag{S.9}$$

where p_j^k is the posterior probability given the current parameter estimates, which is obtained using Bayes' rule as

$$\begin{aligned} p_j^k &= p(z_j^k = 1 | \pi_k, \lambda_k, \boldsymbol{\beta}_k, d_j) \\ &= \frac{\pi_k \lambda_k e^{-\lambda_k d_j}}{\pi_k \lambda_k e^{-\lambda_k d_j} + \frac{1-\pi_k}{P}}. \end{aligned} \tag{S.10}$$

In the M-step, we determine updated values for the parameters π_k, λ_k, and $\boldsymbol{\beta}_k$ by maximizing the expectation Q, which yields

$$\pi_k = \frac{\sum_{j=1}^{M_{t,k}} p_j^k}{M_{t,k}}, \;\; \lambda_k = \frac{\sum_{j=1}^{M_{t,k}} p_j^k}{\sum_{j=1}^{M_{t,k}} p_j^k d_j}, \tag{S.11}$$

and

$$\boldsymbol{\beta}_k = \arg\min_{\boldsymbol{\beta}} \frac{1}{M_{t,k}} \sum_{j=1}^{M_{t,k}} p_j^k d_j(\boldsymbol{\beta}). \tag{S.12}$$

We use the Levenberg-Marquardt (LM) [2] algorithm to solve the optimization problem in (S.12). Starting with an initial estimate of $\boldsymbol{\beta}_k^{(0)}$ (chosen as the identity transformation in our local registration setting), the LM algorithm obtains the optimum on the right-hand-side of (S.12) as the limit of the sequence $\boldsymbol{\beta}_k^{(l+1)} = \boldsymbol{\beta}_k^{(l)} + \boldsymbol{\Delta}$, where $\boldsymbol{\Delta} = [\boldsymbol{\Delta}^u, \boldsymbol{\Delta}^v]$, with $\boldsymbol{\Delta}^u$ and $\boldsymbol{\Delta}^v$ representing the parameter increments for $\boldsymbol{\beta}_k^u$ and $\boldsymbol{\beta}_k^v$, respectively. The parameter increment $\boldsymbol{\Delta}^u$ is obtained by solving the linear equation

$$\left(\sum_{j=1}^{M_{t,k}} \mathbf{J}_j^\intercal \mathbf{J}_j + \sigma \mathbf{E}\right) \boldsymbol{\Delta}^u = 2 \sum_{j=1}^{M_{t,k}} p_j^k r_{j,u}^k \mathbf{J}_j^\intercal, \tag{S.13}$$

where $r_{j,u}^k$ is the u-component of the residual distance vector

$$\mathbf{r}_j^k = \min_i \left(\mathbf{p}_i^{(r,k)} - \tilde{\mathcal{T}}_{\boldsymbol{\beta}_k}\left(\mathbf{p}_j^{(t,k)}\right)\right), \tag{S.14}$$

which can be efficiently obtained from the distance transform [3] and $\mathbf{J}_j$ is the Jacobian of the u-component of the transformation $\tilde{\mathcal{T}}_{\boldsymbol{\beta}_k}\left(\mathbf{p}_j^{(t,k)}\right)$ evaluated at the j^{th} target point $\mathbf{p}_j^{(t,k)}$, which is obtained as

$$\mathbf{J}_j = \frac{\partial\left(\mathbf{a}_j^\intercal \boldsymbol{\beta}_k^u\right)}{\partial \boldsymbol{\beta}_k^u} = \mathbf{a}_j^\intercal, \tag{S.15}$$

$\mathbf{E}$ is the identity matrix, and σ is an iteration dependent damping parameter. If the parameter increment obtained by solving (S.13) leads to an increase in error, then σ is multiplied by a factor of 10. Otherwise, σ is divided by the same factor. The increment $\boldsymbol{\Delta}^v$ is similarly obtained.

S.IV. Visual Results of the Entire Registered Vessel Map

We provide larger images corresponding to the entire registered vessel maps from which smaller regions were presented in the results of Fig. 6 in the main manuscript. Figures S.1 and S.2 show the images from the FLoRI21 [4] and the FIRE [5] datasets, respectively. For consistency, Figs. S.1 and S.2 use the same layout as Fig. 6 in the main manuscript, readers can view the PDF document under high zoom to see individual images or selected regions within the images.

References

[1] L. Ding *et al.*, "Combining feature correspondence with parametric chamfer alignment: Hybrid two-stage registration for ultra-widefield retinal images," submitted for review.

[2] J. Nocedal and S. Wright, *Numerical optimization*. New York, NY, USA: Springer, 2006.

[3] G. Borgefors, "Distance transformations in digital images," *Comp. Vis., Graphics and Image Proc.*, vol. 34, no. 3, pp. 344–371, 1986.

[4] L. Ding *et al.*, "FLoRI21: Fluorescein angiography longitudinal retinal image registration dataset," IEEE Dataport, 2021. [Online]. Available: https://dx.doi.org/10.21227/ydp8-zf19

[5] C. Hernandez-Matas *et al.*, "FIRE: fundus image registration dataset," *Modeling and Artif. Intel. in Ophthalmology*, vol. 1, no. 4, pp. 16–28, 2017.

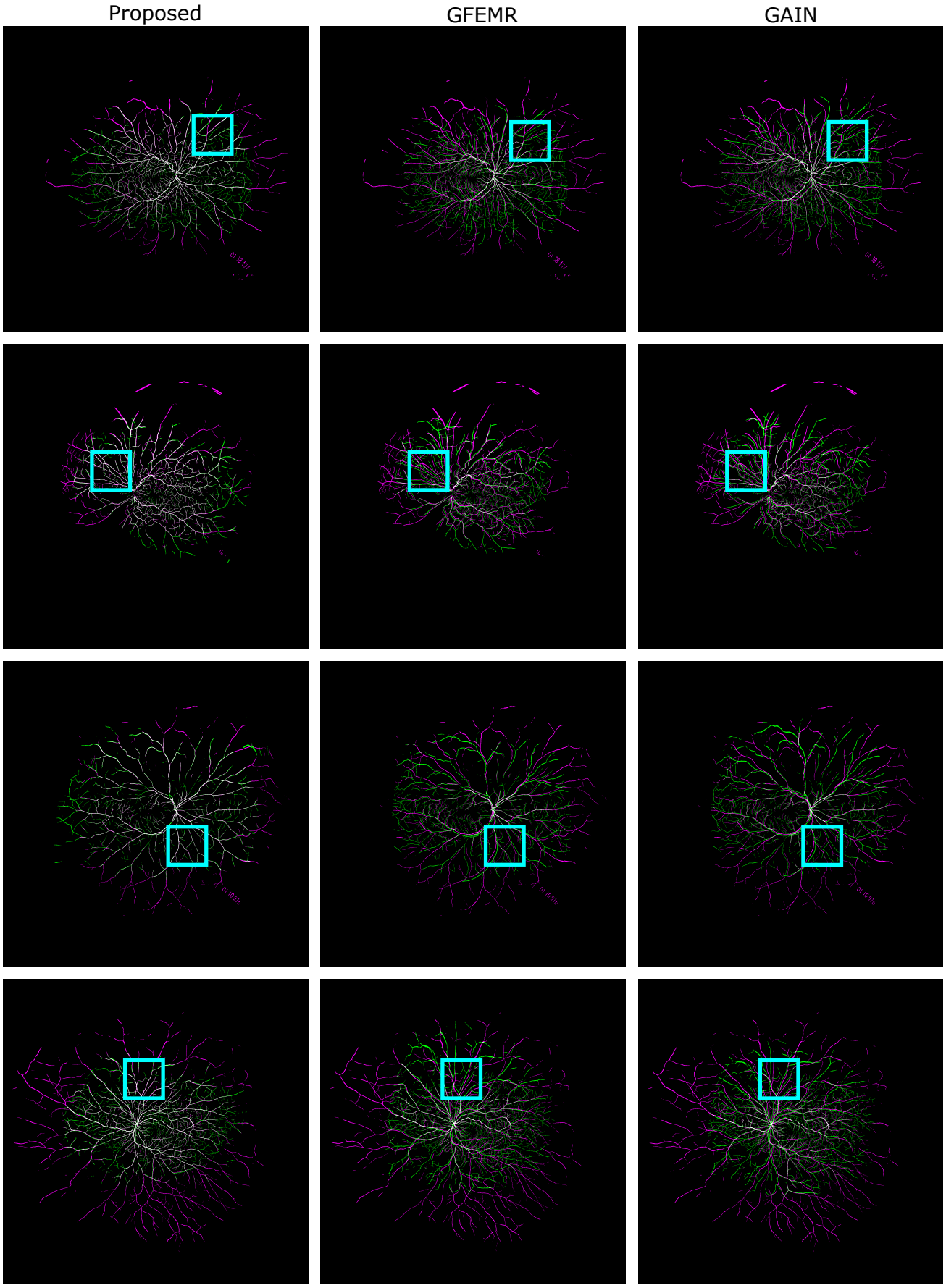

Fig. S.1: Sample registration results for the proposed method and alternative methods on the FLoRI21 dataset. The images are the composition of the reference vessel map (magenta) and the registered target vessel map (green). The regions highlighted by the cyan rectangles are shown in the Fig. 6(a) of the main manuscript.

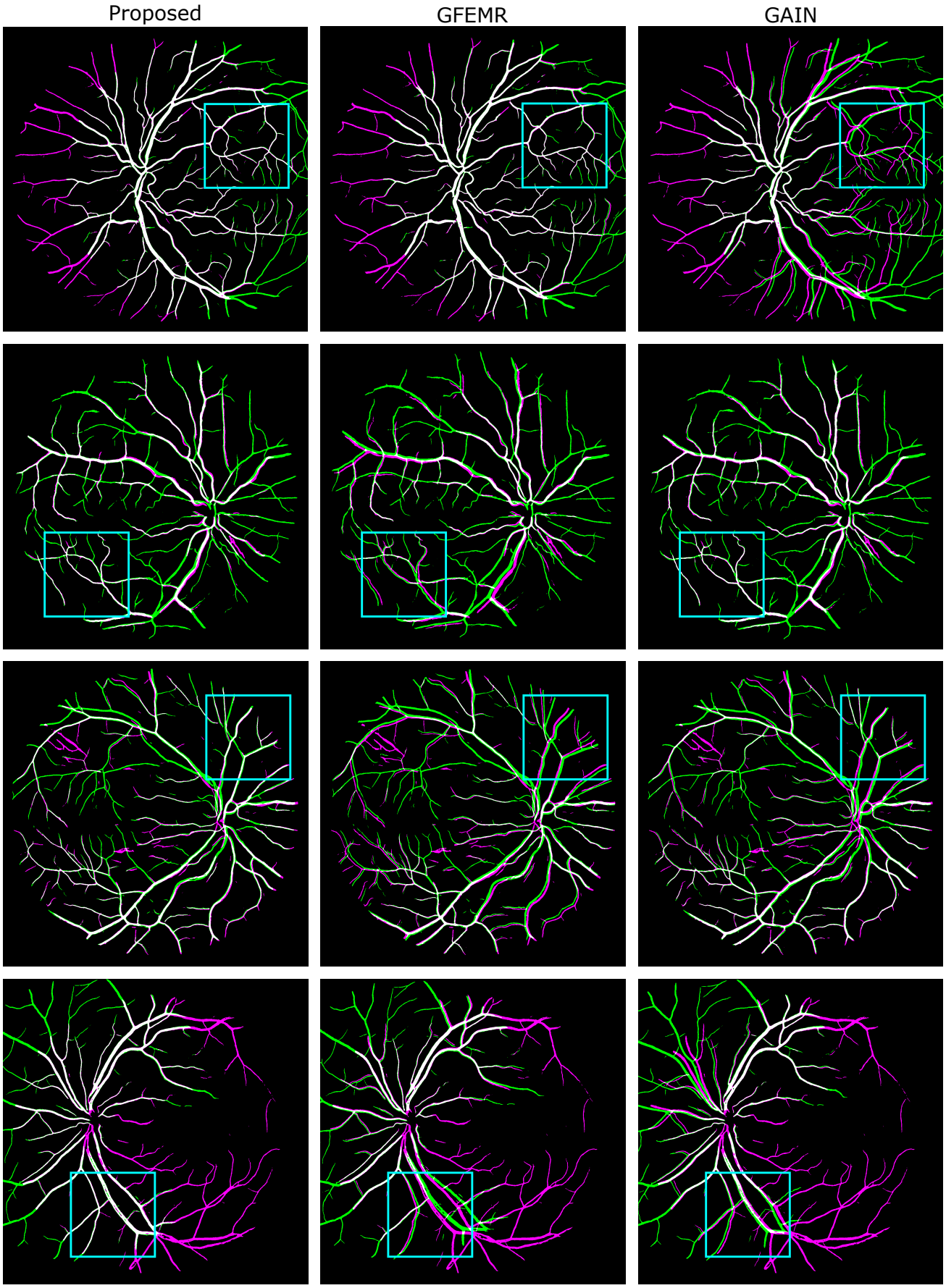

Fig. S.2: Sample registration results for the proposed method and alternative methods on the FIRE dataset. The images are the composition of the reference vessel map (magenta) and the registered target vessel map (green). The regions highlighted by the cyan rectangles are shown in the Fig. 6(b) of the main manuscript.